

Triviality of ϕ_4^4 theory: small volume expansion and new data

Peter Weisz
Max-Planck-Institut für Physik
Föhringer Ring 6
80805 München, Germany

Uli Wolff*
Institut für Physik, Humboldt Universität
Newtonstr. 15
12489 Berlin, Germany

Abstract

We study a renormalized coupling g and mass m in four dimensional ϕ^4 theory on tori with finite size $z = mL$. Precise numerical values close to the continuum limit are reported for $z = 1, 2, 4$, based on Monte Carlo simulations performed in the equivalent all-order strong coupling reformulation. Ordinary renormalized perturbation theory is found to work marginally at $z = 2$ and to fail at $z = 1$. By exactly integrating over the constant field mode we set up a renormalized expansion in z and compute three nontrivial orders. These results reasonably agree with the numerical data at small z . In the new expansion, the universal continuum limit exists as expected from multiplicative renormalizability. The triviality scenario is corroborated with significant precision.

HU-EP-10

MPP-2010-160

SFB/CCP-10-127

*e-mail: uwolff@physik.hu-berlin.de

1 Introduction

The standard view [1], [2] of the primary textbook example of a scalar field theory with quartic self-coupling in four space-time dimensions is that it is a trivial theory. This means that a true continuum limit of the regularized theory inevitably leads to a non-interacting Gaussian theory. More precisely, the perturbative renormalization group predicts that, once one is close to this limit, the renormalized coupling asymptotically vanishes logarithmically with the cutoff. This weak dependence keeps ϕ^4 theory useful as a physical theory, because we can simultaneously have only small cutoff effects but still have sizeable interaction in an effective theory valid over a limited but large range of length scales. In the absence of rigorous proofs of triviality in four dimensions, it remains to follow the strategy of [2] and to verify in a nonperturbative lattice calculation that the perturbative scenario actually applies close to the continuum limit, and thus to exclude the logical possibility that it is simply irrelevant. We re-address this old subject because numerical progress [3] has made it possible to render such tests more stringent with only moderate resources. Although the situation is complicated by the coupling to other fields, triviality is also the standard scenario for the Higgs field in the Standard Model. The subtle nature of logarithmic effects makes a numerical check of the triviality picture rather non-trivial in spite of the simple field structure of ϕ^4 theory. A number of Monte Carlo simulations have been conducted of which [4] is one example where the then new cluster algorithm was used in the symmetric phase. These as well as our new simulations took place in the Ising limit of ϕ^4 theory, which amounts to infinitely strong bare coupling, where we expect to find the strongest possible interaction.

In [3] a novel approach to simulate this model was presented which is based on the simulation of Aizenman's random current representation [5]. Its numerical efficiency is closely related to the fact that this equivalent reformulation enabled Aizenman to derive bounds that prove triviality in $D > 4$ dimensions. For both applications it is essential that the connected four point correlation that enters into the renormalized coupling, can be calculated *without* the need of performing cancellations and with the Lebowitz inequality [6] being manifest. The elimination of the otherwise unavoidable loss of significance in the Monte Carlo allows to rather easily compute the renormalized coupling with per mille precision close to the continuum limit. An additional decisive bonus is the practically complete absence of critical slowing down.

The triviality conjecture in $D = 4$ is investigated here in a finite volume renormalization scheme where the continuum limit is approached on a volume that remains finite in units of the physical renormalized length scale. This has the same advantage here as in asymptotically free theories [7], [8], namely that the mastering of a large ratio of physical scales is avoided and one can thus probe the

universal continuum limit much more closely .

In this paper we employ the numerical technique described in [3] without changes and therefore here leave out all details on this. The data with $z = 2$, already published in [3], are extended by including a lattice of size 64^4 and by simulating two more series of lattices at $z = 1$ and $z = 4$. In addition we report on a computation in lattice perturbation theory that we employ to analyze the data. This calculation goes beyond [2] by allowing for finite z values and by computing the lattice artifacts of the Callan Symanzik β -function up to two loops. By combining with [2] we also obtain the three loop term for various finite z . By comparing with our data we will conclude that perturbation theory works well for large z and fails for small z .

A plausible reason for the failure of perturbation theory on a small torus is that the constant zero momentum mode may receive too little Gaussian damping to justify its perturbative treatment [9]. We therefore embark on an alternative approximation scheme where we treat this one mode exactly while maintaining the perturbative expansion for all others. It turns out that this type of expansion rearranges itself under renormalization to an expansion in powers of z^2 for arbitrary values of g/z^4 . The new expansion is found to be applicable and accurate at small z .

We set up our renormalization scheme in sect. 2. Our perturbative calculation is described in sect. 3 and app. A and numerical results are discussed in sect. 4. The new small volume expansion is outlined in sect. 5 and app. B and we conclude in sect. 6.

2 Finite size renormalization scheme

We define ϕ^4 theory on a four dimensional periodic lattice of extent L in all directions by the standard Euclidean action

$$S = a^4 \sum_x \left\{ \frac{1}{2} \sum_{\mu} (\partial_{\mu} \phi)^2 + \frac{1}{2} m_0^2 \phi^2 + \frac{g_0}{4!} \phi^4 \right\}. \quad (1)$$

Here $\partial_{\mu} \phi(x) = [\phi(x + a\hat{\mu}) - \phi(x)]/a$ is the standard nearest neighbor forward derivative and $\hat{\mu}$ is a unit vector in the μ direction. From here on we mostly use lattice units and leave out powers of $a = 1$ except for some formulas where we find that clarity is gained by restoring explicit factors of a . A completely equivalent form of the above action on the lattice is given by

$$S = -2\kappa \sum_{x,\mu} s(x)s(x + \hat{\mu}) + \sum_x [s(x)^2 + \lambda(s(x)^2 - 1)^2]. \quad (2)$$

The relation between the two parameterizations is given by

$$g_0 = 6\lambda/\kappa^2, \quad m_0^2 = (1 - 2\lambda)/\kappa - 8, \quad \phi = \sqrt{2\kappa}s. \quad (3)$$

In the latter form it becomes manifest that for $\lambda \rightarrow \infty$ the integrations over the spin field $s(x)$ reduce to Ising sums over $s(x) = \pm 1$.

It has become standard [2] to take the continuum limit along vertical lines in the (κ, λ) plane by sending κ to its critical value $\kappa_c(\lambda)$ at fixed λ . If for the infinite volume this limit is taken from below the theory is in the symmetric phase. We adhere to this ‘coordinate choice’ although alternative procedures are conceivable, of course, without however changing the set of continuum theories that can be reached.

It is now a completely well-defined procedure to perturbatively compute, starting from (1) and within the regularized theory, the (bare) effective action¹ as a sum over connected one particle irreducible graphs with propagators for external lines canceled. At first we are interested in the 2-point vertex function $\Gamma^{(2)}(p, -p)$. It is related to the susceptibility measured in simulations by

$$\chi_2 = \sum_x \langle s(0)s(x) \rangle = [-2\kappa\Gamma^{(2)}(0, 0)]^{-1}. \quad (4)$$

For our definition of a renormalized mass m a non-zero momentum is required for which we take the minimal one

$$p_* = (2\pi/L, 0, 0, 0). \quad (5)$$

Then the ‘second moment’ definition of m follows from the universal ratio

$$\frac{\Gamma^{(2)}(0, 0)}{\Gamma^{(2)}(p_*, -p_*)} = \frac{1}{\chi_2} \sum_x e^{-ip_*x} \langle s(0)s(x) \rangle := \left(1 + \frac{\hat{p}_*^2}{m^2}\right)^{-1} \quad (6)$$

with $\hat{p}_\mu = 2 \sin(p_\mu/2)$. In the following we define the finite size continuum limit by holding constant the combination

$$z = mL. \quad (7)$$

Thus for some choice of z (and λ) we consider sequences of lattices with growing $L \equiv L/a \rightarrow \infty$ where for each L we adjust κ such that z has the desired value. We may also say that in this way we have defined a family of renormalization schemes, one for each value of z .

¹The sign of Γ is not uniform in the literature. We follow the convention [2] which leads to $\Gamma^{(2)}(0, 0) = -m_0^2 + O(g_0)$.

The renormalized coupling is now an output observable in this procedure which is given by another universal ratio

$$g = -\frac{\chi_4}{\chi_2^2} m^4 \quad (8)$$

with the connected four point susceptibility

$$\chi_4 = \sum_{x,y,z} \langle s(0)s(x)s(y)s(z) \rangle - 3L^4 \chi_2^2 = \frac{1}{(2\kappa)^2} \frac{\Gamma^{(4)}(0,0,0,0)}{[\Gamma^{(2)}(0,0)]^4} \quad (9)$$

or, equivalently, the 4-point vertex function $\Gamma^{(4)}$. It vanishes for a Gaussian theory and is hence a key quantity in connection with the triviality conjecture. An important property of our coupling is that it is rigorously bounded in the range

$$0 \leq g/z^4 \leq 2. \quad (10)$$

This bound, based on [5], is manifestly visible in eq. (20) of [3] where an observable with values in $\{0,1\}$ is averaged with a positive weight to yield $g/(2z^4)$.

The renormalization scheme in [2] is defined in an infinite volume and uses the ‘zero momentum’ definition for the renormalized mass $m \equiv m_R$. We make contact with this scheme by taking within our family of schemes the simultaneous limit $z \rightarrow \infty, L \rightarrow \infty$ at fixed $m_R = z/L$. In this limit $\hat{p}_*^2/m^2 \simeq (2\pi/z)^2$ becomes arbitrarily small and (6) goes over into (2.12) of [2]. Note that this is not a continuum limit as long as $m_R \equiv am_R$ is finite, in contrast to $L \equiv L/a \rightarrow \infty$ at fixed z .

We are now in a position to define the Callan Symanzik β -function in our scheme by

$$\beta_z(g, a/L) = -L \frac{\partial}{\partial L} g|_{\lambda,z}. \quad (11)$$

As L is integer, the derivative must be approximated by a sufficiently accurate finite difference formula, see sect. 3.1 for further details.

There is a family of ‘curves’ in the $(g, a/L)$ plane, one for each value $\lambda \in [0, \infty)$, on which β_z and other observables become defined. We write ‘curve’ because with only integer L/a it is actually a sequence of discrete points. If the triviality conjecture holds, then all these curves end in the point $(0,0)$. In figure 1 we see a sketch of the expected shape of the domains for $z = 4$ and $z = 2$ based on our nonperturbative data together with continuum extrapolations to be discussed in section 4. The respective domains are the areas under the curves if we assume that smaller λ yield smaller g . An analogous curve for $z = 1$ would be roughly around $g \sim 1.5$ before diving down to zero.

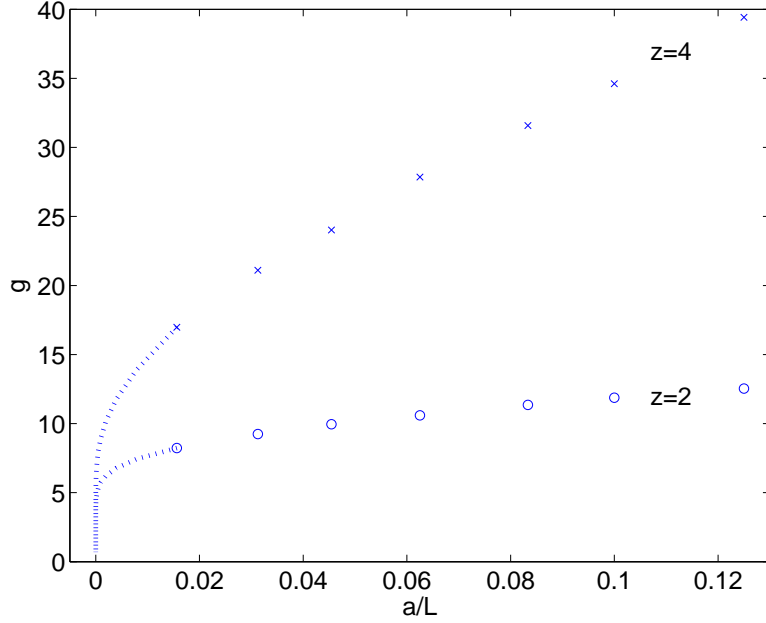


Figure 1: Upper boundaries of the domains of renormalized coupling versus cutoff at $z = 2, 4$. Symbols are Monte Carlo results and 1-loop perturbation theory furnishes the dotted extrapolations.

At tree level of perturbation theory we trivially find $g = g_0$ and $m = m_0$. In terms of the natural variables in (11) this reads however

$$g = \frac{6\lambda}{(1-2\lambda)^2} (8 + z^2/L^2)^2 \quad (12)$$

which leads to

$$\beta_z = \frac{4z^2/L^2}{8 + z^2/L^2} g + O(g^2) \quad (13)$$

as already noticed in [2]. To avoid this tree level lattice artefact in the β -function we change the definition of the renormalized coupling [3] by a term that vanishes quadratically with the cutoff into

$$\tilde{g} = gr^2(z/L) \quad (14)$$

with

$$r(m) = \frac{1}{1 + m^2/8}. \quad (15)$$

The β -function for this renormalized coupling

$$\tilde{\beta}_z(\tilde{g}, a/L) = -L \frac{\partial}{\partial L} \tilde{g}|_{\lambda, z} \quad (16)$$

vanishes at tree level.

3 Lattice perturbation theory up to two loop order

3.1 Artifacts of the one and two loop beta function

In this section we discuss the asymptotic expansion of $\tilde{\beta}_z$ in powers of \tilde{g}

$$\tilde{\beta}_z(\tilde{g}, a/L) = \sum_{l \geq 1} \tilde{b}_z^{(l)}(a/L) \tilde{g}^{l+1} \quad (17)$$

or the completely analogous formula without the tildes [which must include $l = 0$ however]. The (perturbative) renormalizability implies the finiteness of all limits $\lim_{a/L \rightarrow 0} \tilde{b}_z^{(l)}(a/L)$. The one and two loop terms are scheme independent, which here means independent of z , and have the universal values

$$\lim_{a/L \rightarrow 0} \tilde{b}_z^{(1)}(a/L) = \bar{b}^{(1)} = \frac{3}{16\pi^2}, \quad \lim_{a/L \rightarrow 0} \tilde{b}_z^{(2)}(a/L) = \bar{b}^{(2)} = -\frac{17/3}{(16\pi^2)^2}. \quad (18)$$

In [2] the three loop result

$$\tilde{b}_\infty^{(3)}(0) = \bar{b}_\infty^{(3)} = \frac{26.908403}{(16\pi^2)^3} \quad (19)$$

is given for the infinite volume scheme.

In appendix A we derive the coefficients of the following expansion

$$\tilde{g} = \tilde{g}_0 + \tilde{p}_1(z, L) \tilde{g}_0^2 + \tilde{p}_2(z, L) \tilde{g}_0^3 + \mathcal{O}(\tilde{g}_0^4) \quad (20)$$

with

$$\tilde{g}_0 = g_0 r^2(m_0). \quad (21)$$

We have performed the necessary Feynman diagram sums up to $L = 100$. The only technicality that is perhaps worth mentioning here is that by a judicious use of both momentum and position space propagators and the fast Fourier transform we compute all two loop diagrams by performing no more than $\mathcal{O}(L^4 \ln L)$ operations at each L . More details are given in app. A.

Because of the relation $\tilde{g}_0 = 384\lambda/(1 - 2\lambda)^2$ we may keep \tilde{g}_0 constant in (16) instead of λ . Then we obtain

$$\tilde{b}_z^{(1)}(L^{-1}) = -L \frac{\partial}{\partial L} \tilde{p}_1(z, L), \quad \tilde{b}_z^{(2)}(L^{-1}) = -L \frac{\partial}{\partial L} [\tilde{p}_2(z, L) - \tilde{p}_1(z, L)^2]. \quad (22)$$

For several z we have checked that in the Symanzik expansion in terms of $\ln^l LL^{-2n}$ the exact values $\bar{b}^{(1,2)}$ of (18) emerge as leading terms ($l = 1, n = 0$) with significant precision. With this verified we cancel them and form the deviations

$$\delta_z^{(1)}(L) = -\frac{1}{\bar{b}^{(1)}} L \frac{\partial}{\partial L} [\tilde{p}_1(z, L) + \bar{b}^{(1)} \ln L], \quad (23)$$

$$\delta_z^{(2)}(L) = -\frac{1}{\bar{b}^{(2)}} L \frac{\partial}{\partial L} [\tilde{p}_2(z, L) - \tilde{p}_1(z, L)^2 + \bar{b}^{(2)} \ln L]. \quad (24)$$

We use the four point formula for the derivative which contributes errors of order L^{-6} to $\delta_z^{(i)}$ which itself is expected of size $O(L^{-2})$. Results are shown in Fig. 2. The dots are the corresponding lattice sums while the lines are fitted third degree polynomials in L^{-2} to interpolate and represent the data.

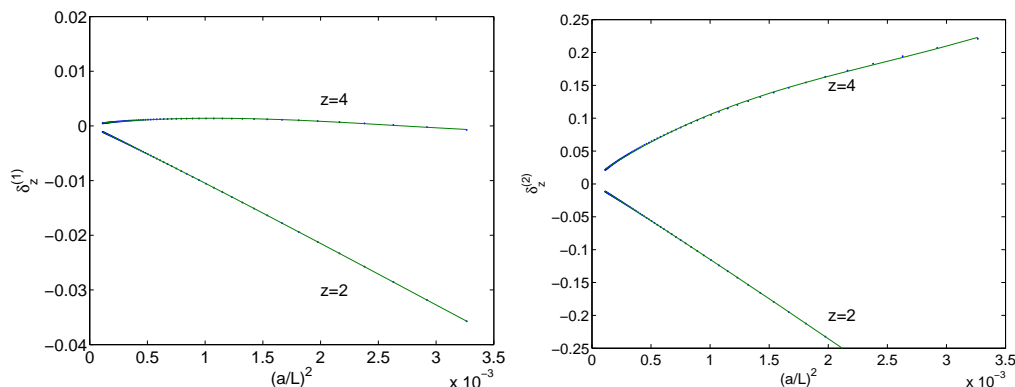


Figure 2: Deviation from the universal values of the 1 and 2-loop β -function at finite lattice spacing.

3.2 Three loop beta function

We now want to relate the renormalized couplings g and g' referring to schemes defined with two values z and z' that we freeze for a while. To appreciate the relation we first give an ‘operational’ description. We first choose a value $L \equiv L/a \gg 1$. Then there are (assumed to be) bare parameters λ, κ in the scaling region that lead to renormalized values $z = mL$ and g . Now *with the bare parameters unchanged* we change $L \rightarrow L' \gg 1$ until z' is found. In this way g' and L'/L become functions of g up to scaling violations of order L^{-2} that we neglect in this subsection. With these relations known the β function transforms as

$$\beta_z(g) = \frac{\partial g}{\partial g'} \beta_{z'}(g'). \quad (25)$$

In the end we shall be interested in the limit $z' \rightarrow \infty$ with $g' \rightarrow g_R$ to make contact with the infinite volume scheme for which we know the 3 loop β function (19).

The relations just described are now analyzed in perturbation theory. Then there is an expansion

$$g = g' + P_1(z, z')g'^2 + P_2(z, z')g'^3 + O(g'^4). \quad (26)$$

From this form it follows that the first two expansion coefficients of the β -functions are independent of z while at three loops the connection is

$$\bar{b}_z^{(3)} - \bar{b}_{z'}^{(3)} = \bar{b}^{(1)}(P_2 - P_1^2) - P_1\bar{b}^{(2)}. \quad (27)$$

Using (88) to leading order we first derive

$$L'/L = z'/z[1 + Q_1(z, z')g' + O(g'^2)] \quad (28)$$

with

$$Q_1(z, z') = \frac{1}{2} \frac{L^2}{z^2} [q_1(z', Lz'/z) - q_1(z, L)] + O(L^{-2}). \quad (29)$$

Then we find

$$P_1(z, z') = p_1 - p'_1 + O(L^{-2}), \quad (30)$$

$$P_2 = p_2 - p'_2 - 2p'_1(p_1 - p'_1) + \bar{b}^{(1)}Q_1 + O(L^{-2}). \quad (31)$$

Here p_i, p'_i denote $p_i(z, L)$ and $p_i(z', Lz'/z)$ respectively. Arguments L' have been eliminated with (28) and use was made of $p_1(z', L') = -\bar{b}^{(1)} \ln L' + O(L^0)$.

We have defined now a number of expansion coefficients that emerge as finite continuum limits as $L \rightarrow \infty$. The Symanzik expansions of the corresponding combinations of lattice Feynman diagrams have been analyzed by the method given in appendix D of [10]. Results are collected in Tab. 1. We see that the 3-loop coefficient $\bar{b}_z^{(3)}$ rises very steeply for $z \lesssim 3$. The negative entries in the last column imply that as one lowers z starting from $z = 16$ (which is effectively infinite) to smaller values, the behavior of $\bar{b}_z^{(3)}$ is not completely monotonic. One might be tempted to think of numerical inaccuracies here, but as far as we can tell, the negative sign seems to be significant. The table allows to change z in cycles for which we find consistency. A rough picture is that $\bar{b}_z^{(3)}$ is constant above $z = 4$ and rises by a factor 15 for $z = 4 \rightarrow 2$ and by another factor 270 for $z = 2 \rightarrow 1$. The typical couplings will at the same time be seen below to diminish by factors of roughly $1/3$ and $1/7$. This means that the 3-loop contribution overall rises steeply compared to the 2-loop term with its z -independent coefficient. In this way the perturbative series indicates its breakdown for small z .

z, z'	$Q_1 \times 10^3$	$P_1 \times 10^3$	$P_2 \times 10^3$	$(\bar{b}_z^{(3)} - \bar{b}_{z'}^{(3)}) \times (4\pi)^6$
1, 2	210.06698	-1394.9977	3437.304	110315.00
2, 4	9.7211061	-80.361921	12.52668	382.0849
4, 8	0.2310329	-2.952908	0.04461	0.0425
8, 16	0.0010522	-0.024524	0.00024	-0.0037
2, 3	8.6999022	-70.199600	10.75077	372.7864
3, 6	1.2399938	-12.901805	0.44644	9.4008
6, 12	0.0132854	-0.237614	0.00203	-0.0651
4, 6	0.2187899	-2.739483	0.04164	0.1022
8, 12	0.0010424	-0.024189	0.00022	-0.0053

Table 1: Expansion coefficients relating renormalization schemes defined by z and z' respectively. Numerical errors are beyond the digits quoted.

4 Analysis of precise numerical data

As mentioned in the introduction, our simulations here follow in all details those described in [3]. In particular, for each set of parameters we have generated a statistics of 10^6 iterations resulting in per mille errors. Due to the efficiency of the method this could be done in a short time on a few up-to-date PCs.

In the next subsections we list data and plot couplings versus cutoff for $z = 4, 2, 1$. The tables contain the quantity \mathcal{X} that is related to the coupling by

$$g = 2z^4 \mathcal{X}. \quad (32)$$

The evolutions of the coupling are compared with curves obtained by integrating the renormalization group equation

$$L \frac{\partial \tilde{g}}{\partial L} = -\tilde{\beta}_z(\tilde{g}, 0) \quad (33)$$

starting from the ‘measured’ coupling at the largest $L/a = 64$. The (solid) curves labelled with a loop order refer to the perturbative expansion of $\tilde{\beta}_z$. We have also looked at the curves including the known one and two loop cutoff effects, i.e. with $\tilde{\beta}_z(\tilde{g}, 1/L)$ on the right hand side. We find however that these small corrections do not systematically improve the picture. Sometimes they go in the right and sometimes in the wrong direction. We below offer a possible explanation for this and do not include these curves in the plots. For the case $z = 2$ they are visualized however (without $L = 64$) in Fig. 2 of [3]. Instead we here include additional curves (dashed) labelled LO, NLO, NNLO. They refer to the leading, next-to-leading and next-to-next-to-leading orders of the small volume expansion that is explained in detail in section 5.

4.1 $z = 4$

L/a	2κ	z	\mathcal{X}	$\partial\mathcal{X}/\partial z$	$\mathcal{X}(z = 4)$
8	0.141976	4.0025(22)	0.07684(29)	-0.0556(5)	0.07698(27)
10	0.144491	3.9956(21)	0.06783(27)	-0.0518(5)	0.06760(25)
12	0.145933	3.9991(20)	0.06173(26)	-0.0489(5)	0.06168(24)
16	0.147481	4.0045(19)	0.05419(24)	-0.0441(5)	0.05439(23)
22	0.148454	4.0004(18)	0.04690(22)	-0.0387(5)	0.04691(21)
32	0.1490781	4.0002(17)	0.04120(21)	-0.0360(5)	0.04121(20)
64	0.1495244	4.0009(15)	0.03314(18)	-0.0292(7)	0.03316(18)

Table 2: Monte Carlo results for $z = 4$.

Data for $z = 4$ are tabulated in Tab. 2 and plotted in Fig. 3. At this z value perturbation theory works as one expects: the successive terms alternate around the nonperturbative answer and get closer to it. The change in the coupling as the cutoff changes from $L/a = 64$ to $L/a = 32$ is reproduced with 1.1% error in the 3-loop approximation (2.4% and 3.9% for 2- and 1-loop). In the small volume expansion LO and NLO fall almost on top of each other and are close to 1-loop while NNLO is not far from the 2-loop result.

4.2 $z = 2$

L/a	2κ	z	\mathcal{X}	$\partial\mathcal{X}/\partial z$	$\mathcal{X}(z = 2)$
8	0.148320	1.9981(27)	0.39235(96)	-0.3200(14)	0.39175(63)
10	0.148748	1.9949(26)	0.37256(92)	-0.3193(14)	0.37093(62)
12	0.148996	1.9992(26)	0.35493(91)	-0.3165(15)	0.35469(60)
16	0.149270	1.9988(25)	0.33161(91)	-0.3129(16)	0.33125(58)
22	0.149449	2.0085(24)	0.30831(86)	-0.3030(16)	0.31088(57)
32	0.149571	1.9956(24)	0.29028(83)	-0.2993(20)	0.28896(55)
64	0.1496564	1.9893(22)	0.26016(78)	-0.2887(27)	0.25706(51)

Table 3: Monte Carlo results for $z = 2$.

Data for $z = 2$ are tabulated in Tab. 3 and plotted in Fig. 4. For $z = 2$ the one loop result happens to be exact within errors (0.2%), while 2- and 3-loop are off by 1.4% and 3.9% respectively for the same benchmark as discussed in the previous subsection. As already concluded in [3] this is a limiting case for perturbation theory as an asymptotic expansion, where higher loops do not help at all any

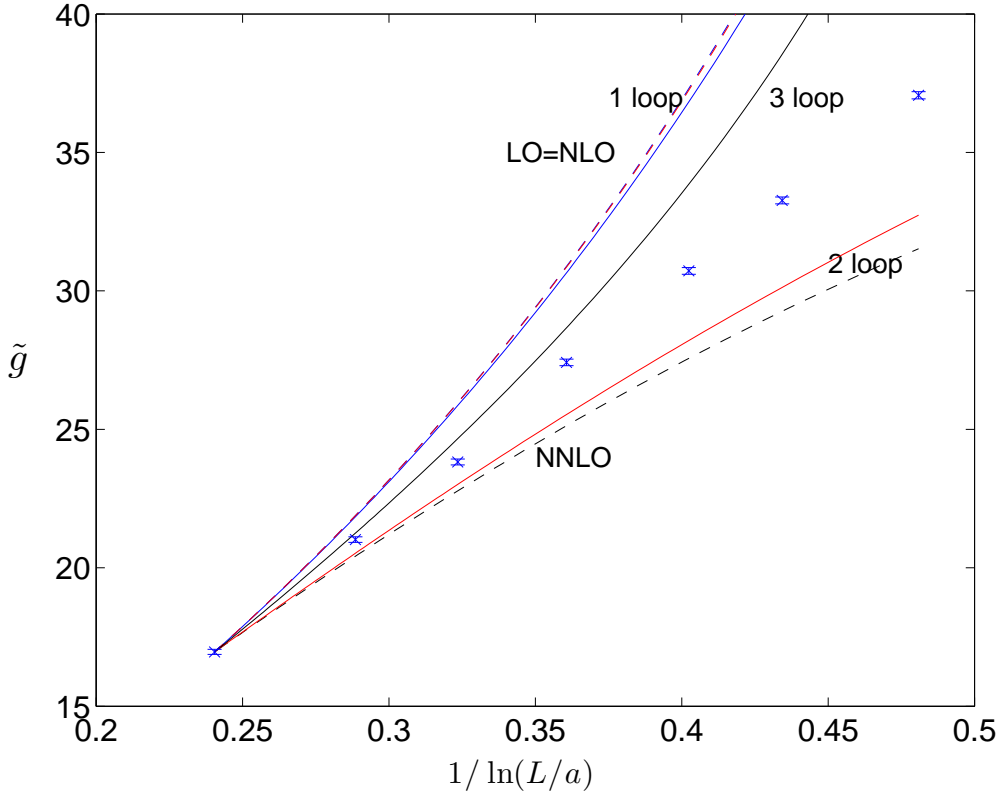


Figure 3: Evolution of the coupling \tilde{g} with the cutoff L/a for $z = 4$.

more. The precision of the small volume expansion is 2.6%, 2.4%, 1.0% for LO, NLO, NNLO respectively.

4.3 $z = 1$

Data for $z = 1$ are tabulated in Tab. 4 and plotted in Fig. 5. At $z = 1$ perturbation theory is not useful anymore. The coupling itself (but not g/z^4 on its natural scale) has small values and therefore the 2-loop contribution, whose coefficient cannot depend on z , is tiny. The very large 3-loop term knocks the approximation far to the other side. The small volume expansion exhibits deviations of 0.7%, 0.5%, 0.3% for LO, NLO, NNLO.

4.4 Lattice artifacts and perturbation theory

In this subsection we offer a short discussion whether or not we expect the lattice artifacts to be well represented by perturbation theory. This may be questionable

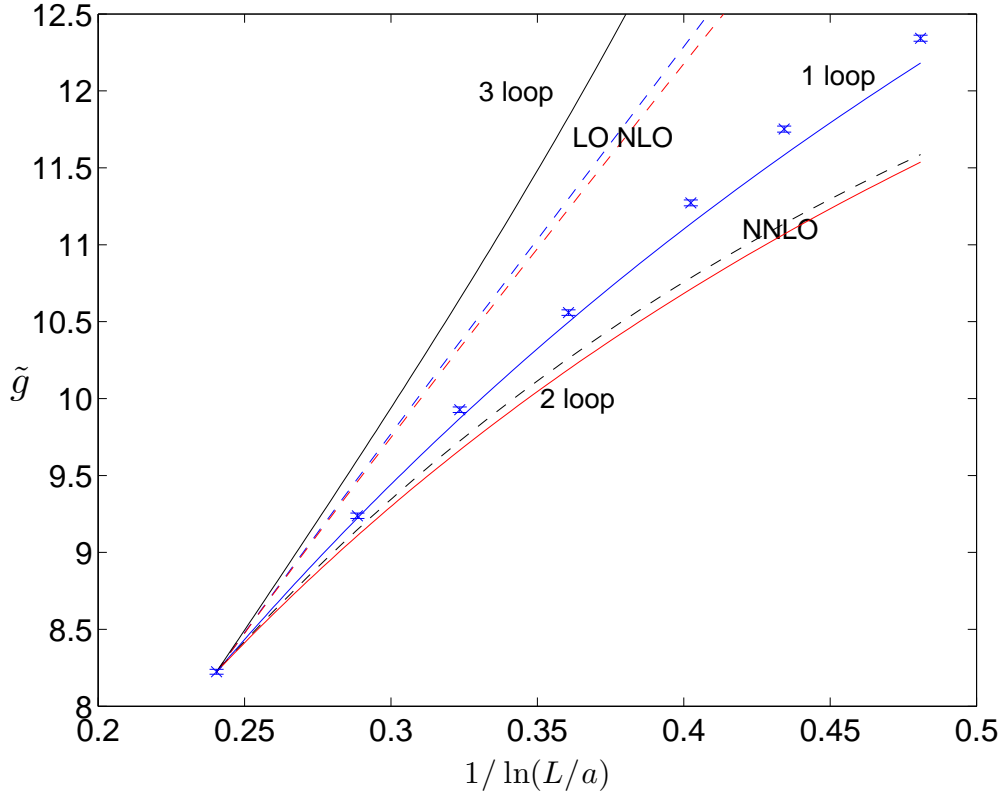


Figure 4: Evolution of the the coupling \tilde{g} with the cutoff L/a for $z = 2$.

even in the regime where the continuum behavior *is* reproduced.

We want to analyze closer the perturbative procedure that we have applied, which is however the conventional one. To derive the expansion coefficients (17) we consider g_0 as an arbitrarily small expansion parameter and correspondingly expand around $\phi \equiv 0$ in (1). Then we re-expand the truncated series in the renormalized coupling g or \tilde{g} . This series is then held against lattice data produced with λ or g_0 such that the *bare* lattice action has a pair of nonzero constant minima. This is so in the most extreme way for the Ising limit. Renormalized perturbation theory is expected to describe the universal physics in spite of the apparent contradiction as long as successive terms in the g expansion (at small a/L) look reasonably ‘convergent’. A possible explanation is as follows. We may simultaneously consider a lattice that is coarser but still in the scaling region tuned to the same (matched) renormalized parameters. On this lattice the bare g_0 will be smaller and the expansion may also be *naively* justified. Up to differing small scaling violations the universal physics will then agree on both lattices.

L/a	2κ	z	\mathcal{X}	$\partial\mathcal{X}/\partial z$	$\mathcal{X}(z=1)$
8	0.151670	1.0020(25)	0.79953(84)	-0.4444(30)	0.80040(85)
10	0.150900	0.9997(24)	0.78776(88)	-0.4641(30)	0.78764(83)
12	0.150498	0.9999(24)	0.77930(92)	-0.475(30)	0.77926(82)
16	0.150118	1.0032(22)	0.76121(96)	-0.5074(31)	0.76281(80)
22	0.149907	0.9961(22)	0.75058(101)	-0.5213(32)	0.74854(78)
32	0.149787	1.0032(21)	0.72936(106)	-0.5436(50)	0.73110(75)
64	0.1497143	0.9993(20)	0.70179(110)	-0.5797(48)	0.70141(71)

Table 4: Monte Carlo results for $z = 1$.

One could consider the extension of this matching to the leading cutoff effects in the spirit of the Symanzik effective action. But then one would need further improvement terms on the coarser lattice to reproduce the cutoff effects of the finer one. As an alternative qualitative argument we could imagine a block-spin coarsening of the original lattice. Then we would expect to arrive at an effective action on the coarse lattice consisting of the relevant terms of (1) with small g_0 and additional contributions corresponding to Symanzik terms. Therefore the relation between cutoff effects computed in perturbation theory with the standard action (1) as sketched above and those of the nonperturbative results may not be so straightforward in our opinion.

5 Small volume perturbation theory

In this section we introduce a modified perturbative expansion which will turn out to lead to a systematic expansion in the finite size scaling variable z defined in (7).

In our perturbative calculation the Gaussian damping of the low momentum modes on the torus is controlled by $\omega^2 \cong m_0^2 + (2\pi/L)^2 \vec{n}^2$ with \vec{n} having small integer components. For small z with $m_0 = z/L + \mathcal{O}(g_0)$ the $\vec{n} = 0$ mode receives little damping and ordinary perturbation theory may be a bad starting point [9]. We therefore split up the lattice field

$$\phi(x) = \frac{1}{Lg_0^{1/4}}\bar{\phi} + \eta(x), \quad \sum_x \eta(x) = 0. \quad (34)$$

We decompose the action (1) into three parts, $S = S_{0,\bar{\phi}} + S_{0,\eta} + S_1$,

$$S_{0,\bar{\phi}} = \frac{1}{2}z_0^2\bar{\phi}^2 + \frac{1}{4!}\bar{\phi}^4, \quad (35)$$

$$S_{0,\eta} = \frac{1}{2} \sum_{x,\mu} \left\{ (\partial_\mu \eta)^2 + g_0^{1/2} \frac{2z_0^2 + \bar{\phi}^2}{2L^2} \eta^2 \right\} \quad (36)$$

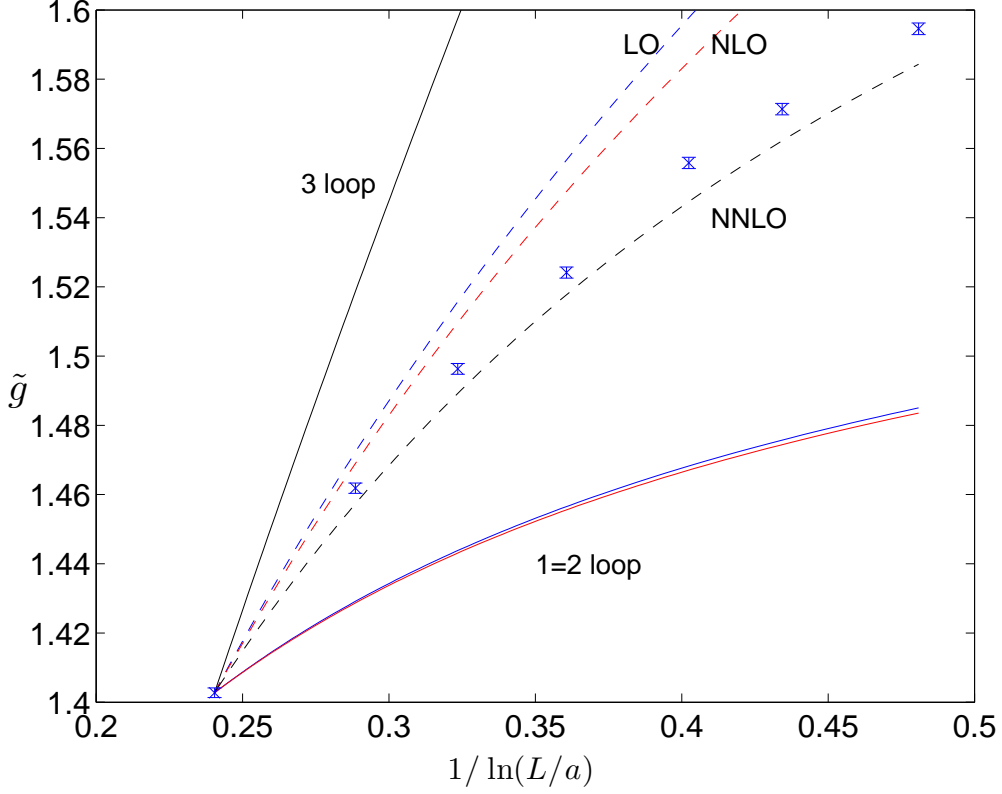


Figure 5: Evolution of the coupling \tilde{g} with the cutoff L/a for $z = 1$.

and

$$S_1 = \sum_x \left\{ \frac{g_0^{3/4}}{3!L} \bar{\phi} \eta^3 + \frac{g_0}{4!} \eta^4 \right\} \quad (37)$$

with

$$z_0^2 = \frac{L^2 m_0^2}{\sqrt{g_0}}. \quad (38)$$

For every cutoff L/a we consider now z_0^2, g_0 as bare input and want to compute from them z and g . The idea is to treat S_0 exactly and S_1 as a perturbation, i.e. g_0 is small at finite z_0^2 . In the end the propagator implied by (36) will also be expanded in $g_0^{1/2}$. Alternatively it could be included as a two η vertex in S_1 from the beginning which we found less efficient however.

The second moment renormalized mass definition (6) implies

$$\frac{z^2}{1 + z^2/K_L} = \sqrt{g_0} \frac{\hat{p}_*^2 \tilde{\Delta}(p_*)}{\langle \bar{\phi}^2 \rangle} \quad (39)$$

with

$$K_L = L^2 \hat{p}_*^2 = 4\pi^2 - \frac{4\pi^4}{3L^2} + \mathcal{O}(L^{-4}). \quad (40)$$

and

$$\tilde{\Delta}(p) = \sum_x e^{-ipx} \langle \eta(0) \eta(x) \rangle. \quad (41)$$

By doing perturbation theory in $\sqrt{g_0}$ we first produce the coefficients of the expansions

$$g/z^4 = 3 - \frac{\langle \bar{\phi}^4 \rangle}{(\langle \bar{\phi}^2 \rangle)^2} = \sum_{n \geq 0} c_n(z_0^2, L) g_0^{n/2} \quad (42)$$

and from (39)

$$z^2 = \sqrt{g_0} \sum_{n \geq 0} d_n(z_0^2, L) g_0^{n/2}. \quad (43)$$

The β function is computed as

$$\beta_z = -L \frac{\partial g}{\partial L} \Big|_{z, g_0}. \quad (44)$$

For the derivative we use

$$L \frac{\partial}{\partial L} \Big|_{z, g_0} = L \frac{\partial}{\partial L} - \rho(z_0^2, L) \frac{\partial}{\partial z_0^2} \quad (45)$$

where all partial derivatives on the right hand side are now taken with respect to the set (z_0, L, g_0) and

$$\rho(z_0^2, L) = L \frac{\partial z^2}{\partial L} \left[\frac{\partial z^2}{\partial z_0^2} \right]^{-1} \quad (46)$$

has been introduced.

If we invert (43) to express $\sqrt{g_0}$ as a series in z^2 we obtain

$$g/z^4 = \sum_{n \geq 0} e_n(z_0^2, L) z^{2n} \quad (47)$$

from (42) and we arrive at the intermediate form

$$\beta_z = z^6 \sum_{n \geq 0} f_n(z_0^2, L) z^{2n}. \quad (48)$$

Below we now refer to results whose derivation is described in some detail in appendix B.

The first coefficients e_0, e_1 are given by

$$e_0 = 3 - \frac{\mu_4}{\mu^2} = 3 \frac{\mu^2 + 2\mu z_0^2 - 2}{\mu^2} \quad (49)$$

and

$$e_1 = -\frac{3C_1}{2\mu^2} \{ \mu^3 z_0^2 + 2\mu^2(3z_0^4 - 2) - 18\mu z_0^2 + 12 \} \equiv \frac{1}{2}\mu C_1 \frac{\partial}{\partial z_0^2} e_0 \quad (50)$$

with the second moment computed with (35)

$$\mu(z_0^2) = \langle \bar{\phi}^2 \rangle_{0,\phi} \quad (51)$$

and the constant C_1 defined in (100). For given g, z we solve for \bar{z}_0^2 in

$$g/z^4 = e_0(\bar{z}_0^2) \quad (52)$$

which gives \bar{z}_0 the status of a renormalized parameter. One finds for example $\bar{z}_0^2 \approx 0.303$ ($\mu \approx 1.25$) for $g = 10, z = 2$. The bare quantity z_0^2 is then written as a power series in z^2 by solving (47)

$$z_0^2 = \bar{z}_0^2 + \sum_{n \geq 1} h_n(\bar{z}_0^2, L) z^{2n}. \quad (53)$$

The lowest order terms are

$$h_1 = -e_1 \left[\frac{\partial e_0}{\partial z_0^2} \right]^{-1} = -\frac{1}{2}\mu C_1, \quad (54)$$

$$h_2 = - \left[e_2 + h_1 \frac{\partial e_1}{\partial z_0^2} + \frac{1}{2} \frac{\partial^2 e_0}{\partial (z_0^2)^2} h_1^2 \right] \left[\frac{\partial e_0}{\partial z_0^2} \right]^{-1}, \quad (55)$$

$$h_3 = - \left[e_3 + h_1 \frac{\partial e_2}{\partial z_0^2} + \frac{h_1^2}{2} \frac{\partial^2 e_1}{\partial (z_0^2)^2} + \frac{h_1^3}{6} \frac{\partial^3 e_0}{\partial (z_0^2)^3} + \frac{\partial^2 e_0}{\partial (z_0^2)^2} h_1 h_2 + h_2 \frac{\partial e_1}{\partial z_0^2} \right] \left[\frac{\partial e_0}{\partial z_0^2} \right]^{-1} \quad (56)$$

with all quantities on the right hand sides taken at \bar{z}_0^2 . To finally obtain the β function in the form which is expected to possess a continuum limit we eliminate z_0^2 from (48) to obtain

$$\beta_z(g) = z^8 (B_1 + B_2 z^2 + B_3 z^4) + O(z^{14}) \quad (57)$$

where the B_k are functions of g/z^4 (via \bar{z}_0^2) only after neglecting lattice artifacts proportional to L^{-2} . This also is the reason why there is no $O(z^6)$ contribution, since

$$f_0 = O(L^{-2}) \quad (58)$$

holds. This can be understood by noting that the leading order $g_0^{1/2}$ correction is essentially a mass renormalization, the term proportional to $\bar{\phi}^2$ in (99). This leads to relations

$$c_1 = \frac{1}{2} C_1 \frac{dc_0}{dz_0^2}, \quad d_1 = \frac{1}{2} C_1 \frac{dd_0}{dz_0^2} - \frac{\mu^2 + 2z_0^2 \mu - 2}{2K_L \mu^2} \quad (59)$$

and also to the last equality in (50). With these identities the cancellation that leaves only cutoff effects for f_0 can be shown. The first three B_k are

$$B_1 = f_1 + h_1 \frac{\partial f_0}{\partial z_0^2}, \quad (60)$$

$$B_2 = f_2 + h_1 \frac{\partial f_1}{\partial z_0^2} + h_2 \frac{\partial f_0}{\partial z_0^2} + \frac{1}{2} h_1^2 \frac{\partial^2 f_0}{\partial (z_0^2)^2}, \quad (61)$$

$$B_3 = f_3 + h_1 \frac{\partial f_2}{\partial z_0^2} + \frac{h_1^2}{2} \frac{\partial^2 f_1}{\partial (z_0^2)^2} + \frac{h_1^3}{6} \frac{\partial^3 f_0}{\partial (z_0^2)^3} + h_1 h_2 \frac{\partial^2 f_0}{\partial (z_0^2)^2} + h_2 \frac{\partial f_1}{\partial z_0^2} + h_3 \frac{\partial f_0}{\partial z_0^2} \quad (62)$$

where the limits $L \rightarrow \infty$ are understood on the right hand sides. It turns out that these combinations are such, that all divergences cancel and only finite universal results enter into the continuum limits of the B_k , see app. B for more details.

Our first result is

$$B_1 = -\frac{9}{16\pi^2} \frac{\mu^3 \bar{z}_0^2 + 2\mu^2(3\bar{z}_0^4 - 2) - 18\mu\bar{z}_0^2 + 12}{\mu^2 + 6\mu\bar{z}_0^2 - 6}. \quad (63)$$

For large \bar{z}_0^2 the fluctuations of $\bar{\phi}$ become Gaussian and μ may be expanded as in (118). We then find the leading large \bar{z}_0^2 behavior

$$e_0 \simeq \frac{1}{\bar{z}_0^4}, \quad B_1 \simeq \frac{3}{16\pi^2} \frac{1}{\bar{z}_0^8}, \quad z^8 B_1 \simeq \bar{b}_1 g^2 \quad (\bar{z}_0^2 \rightarrow \infty) \quad (64)$$

such that in this limit we recover the perturbative result with the one loop coefficient (18). More generally we may run \bar{z}_0^2 through some range and parametrically generate the graph of B_1 versus g/z^4 as shown in Fig. 6.

In the next order we find

$$B_2 = -\frac{4}{9} B_1^2. \quad (65)$$

At the moment we see this form on the basis of our series expansion for B_2 and cannot give a simple reason for this simple relation. In the perturbative limit we thus obtain $B_2 z^{10} \simeq -(4/9) \bar{b}_1^2 g^4 / z^6$ which is a contribution that in ordinary perturbation theory could only come at the 3-loop level.

Finally we find

$$B_3 = -\frac{B_1}{16\pi^2} \left[\frac{1}{4\pi^2} R_3 + \frac{17}{9} \mu^2 \right] \quad (66)$$

with

$$R_3 = \frac{1}{(\mu^2 + 6\mu\bar{z}_0^2 - 6)^2} \times \{ \mu^8 + 16\mu^7 \bar{z}_0^2 + 4\mu^6(20\bar{z}_0^4 - 1) + 4\mu^5 \bar{z}_0^2(24\bar{z}_0^4 - 13) \\ - 16\mu^4(9\bar{z}_0^8 + 3\bar{z}_0^4 + 4) + 48\mu^3 \bar{z}_0^2(15\bar{z}_0^4 - 7) - 228\mu^2(5\bar{z}_0^4 - 1) \\ + 1296\mu\bar{z}_0^2 - 432 \}. \quad (67)$$

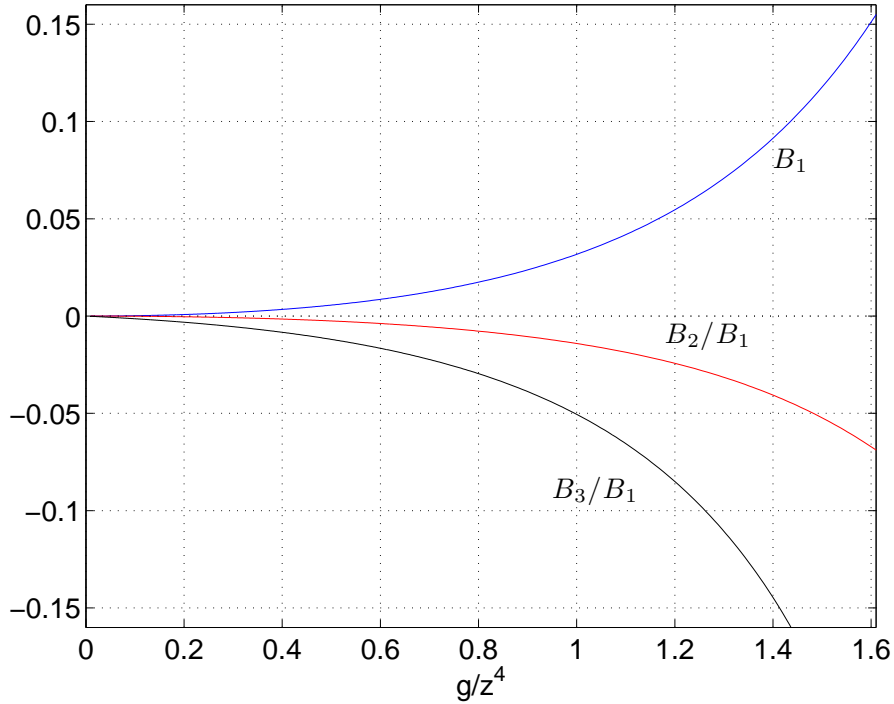


Figure 6: Curves of B_1 , B_2/B_1 and B_3/B_1 versus g/z^4 produced by varying \bar{z}_0^2 between 10 and -1.2 .

Also these factorizations have been found by inspection only. The perturbative limit

$$R_3 \simeq -\frac{4}{\bar{z}_0^8} \quad (\bar{z}_0^2 \rightarrow \infty) \quad (68)$$

yields $B_3 z^{12} \simeq \bar{b}_2 g^3$ with the term with R_3 not contributing to the leading order. We thus recover the 2-loop term (18).

The running with the leading (LO, B_1), next-to-leading (NLO, $B_{1,2}$) and next-to-next-to-leading (NNLO, $B_{1,2,3}$) order β function in the small volume expansion is shown by the dashed lines in Figs. 3 , 4 and 5.

6 Conclusions

We have reported and discussed data for a reasonably defined renormalized coupling g in ϕ^4 theory in finite size systems with $z = 1, 2, 4$ on lattices up to 64^4 . All simulations took place at infinite bare coupling. The dependence of g on the cutoff a/L at $z = 4$ was found to be well described by perturbation theory with the first three loop orders becoming successively more accurate. Thus there is all reason to

trust the perturbative continuation of these curves all the way to vanishing lattice spacing a which implies triviality. At $z = 2$ on the other hand it was already found in [3] that a (presumably accidental) excellent agreement of the nonperturbative evolution with the one loop approximation holds, but that it only deteriorates when further terms are included. We now have added the finding that at $z = 1$ the standard perturbative description fails completely.

The suspicion that the constant mode on the torus is the culprit responsible for the failure has led us to work out an expansion where this one mode is treated nonperturbatively. Upon renormalization this has led us to an expansion of the β function in powers of z itself for finite values of g/z^4 for which we rigorously know that their domain is contained in the interval $[0, 2]$. We construct completely explicitly the first three orders of this expansion, neglecting only order z^{14} and higher, and find it to work very well at our smaller z values. Since this approximation also yields a positive β function, the coupling evolution may be continued to vanishing a and triviality follows once more. The intermediate value $z = 2$ seems somewhat problematic for both expansions and one loop truncated perturbation theory happens to be better than the z -expansion in this difficult range which was unerringly chosen as the first application of the new simulation technique in [3].

We end on a more general remark. Many structural properties of quantum fields theory like renormalizability and the existence of the continuum limit are (in favorable cases) based on proofs to all orders of perturbation theory. It is not so often emphasized, that for nonperturbative calculations on the lattice one has to assume that this holds true also beyond perturbation theory, although we know that the latter can become numerically completely irrelevant, even if one has command over high orders. In our small volume expansion which may perhaps be seen as capturing a glimpse of nonperturbative behavior in an analytic treatment, we could confirm these standard assumptions.

Acknowledgments. We thank Jean Zinn-Justin for discussions in the early stage of this project. U. W. has enjoyed hospitality and support by the Max Planck (Werner Heisenberg) Institut in München. Financial support of the DFG via SFB transregio 9 is acknowledged.

A Perturbative expansion

We here report details on the computation of $\tilde{p}_{1,2}(z, L)$ entering in section 3. In terms of 1PI vertex functions our renormalized parameters read

$$Z^{-1} = [\Gamma^{(2)}(0, 0) - \Gamma^{(2)}(p_*, -p_*)]/\hat{p}_*^2, \quad (69)$$

$$m^2 = -Z\Gamma^{(2)}(0, 0), \quad (70)$$

$$g = -Z^2 \Gamma^{(4)}(0, 0, 0, 0) \quad (71)$$

with the wave function renormalization factor Z and all quantities at finite L . Standard bare perturbation theory gives

$$\Gamma^{(2)}(p, -p) = -m_0^2 - \hat{p}^2 - g_0 \frac{1}{2} J_1 + g_0^2 \frac{1}{4} J_1 H_1 + g_0^2 \frac{1}{6} J_2(m_0^2, p) + O(g_0^3), \quad (72)$$

$$\Gamma^{(4)}(0, 0, 0, 0) = -g_0 + g_0^2 \frac{3}{2} H_1 - g_0^3 \left(3H_{2a} + \frac{3}{4} H_{2b} + \frac{3}{2} H_{2c} \right) + O(g_0^3). \quad (73)$$

The capital letters stand for the usual Feynman diagrams for the two and four point functions up to two loops. With all external lines at zero momentum except in $J_2(m_0^2, p)$ they are regarded as functions of m_0^2 (and L) at this stage. Their actual evaluation proceeds via the following sequence of steps,

$$\tilde{G}(p) = \frac{1}{\hat{p}^2 + m_0^2}, \quad (74)$$

$$G(x) = \frac{1}{L^4} \sum_p e^{ipx} \tilde{G}(p), \quad (75)$$

$$J_1(m_0^2) = G(0), \quad (76)$$

$$H_1(m_0^2) = \frac{1}{L^4} \sum_p [\tilde{G}(p)]^2 = \sum_x [G(x)]^2 \quad (\text{Plancherel}). \quad (77)$$

The momentum sums run over all values $p_\mu = 2\pi n_\mu / L$, $n_\mu = 0, 1, 2, \dots, L-1$. Next we compute

$$\widetilde{G}^n(p) = \sum_x [G(x)]^n e^{-ipx}, \quad n = 2, 3, \quad (78)$$

and use it in

$$H_{2a}(m_0^2) = \frac{1}{L^4} \sum_p \widetilde{G}^2(p) [\tilde{G}(p)]^2, \quad (79)$$

$$H_{2b}(m_0^2) = [\widetilde{G}^2(0)]^2 = H_1(m_0^2)^2, \quad (80)$$

$$H_{2c}(m_0^2) = J_1 \frac{1}{L^4} \sum_p [\tilde{G}(p)]^3, \quad (81)$$

$$J_2(m_0^2, p) = \widetilde{G}^3(p). \quad (82)$$

The Fourier transformations are performed as FFT on one coordinate direction after another, schematically like

$$\tilde{G}(p) \equiv F(p_0, p_1, p_2, p_3) \rightarrow F'(x_0, p_1, p_2, p_3) \rightarrow F''(x_0, x_1, p_2, p_3) \rightarrow \dots \rightarrow G(x) \quad (83)$$

at a total computational complexity of $DL^4 \ln L$ only.

With these expressions we can write (omitting the remainders. . . + $O(g_0^3)$)

$$Z = 1 + \frac{g_0^2}{6\hat{p}_*^2} [J_2(m_0^2, p_*) - J_2(m_0^2, 0)]. \quad (84)$$

and

$$\Delta m^2 = m_0^2 - m^2 = -\frac{g_0}{2} J_1 + \frac{g_0^2}{4} J_1 H_1 + \frac{g_0^2}{6} [(1 + m_0^2/\hat{p}_*^2) J_2 - (m_0^2/\hat{p}_*^2) J_2(m_0^2, p_*)] \quad (85)$$

$$g = g_0 - g_0^2 \frac{3}{2} H_1 + g_0^3 \left(3H_{2a} + \frac{3}{4} H_{2b} + \frac{3}{2} H_{2c} + \frac{1}{3\hat{p}_*^2} [J_2(m_0^2, p_*) - J_2] \right). \quad (86)$$

In these expressions the mass is still m_0 in all diagrams. In order to obtain g as a function of g_0 and m^2 we have to combine the last two lines to eliminate m_0^2 on the right hand sides. To the order considered and using

$$\frac{dJ_1}{dm_0^2} = -H_1, \quad J_1 \frac{dH_1}{dm_0^2} = -2H_{2c} \quad (87)$$

we arrive at

$$\Delta m^2 = q_1(z, L) g_0 + q_2(z, L) g_0^2 \quad (88)$$

with

$$q_1(z, L) = -\frac{1}{2} J_1(m^2) \quad (89)$$

$$q_2(z, L) = \frac{1}{6} [(1 + m^2/\hat{p}_*^2) J_2(m^2, 0) - (m^2/\hat{p}_*^2) J_2(m^2, p_*)], \quad (90)$$

and then

$$g = g_0 + p_1(z, L) g_0^2 + p_2(z, L) g_0^3 \quad (91)$$

with

$$p_1(z, L) = -\frac{3}{2} H_1(m^2), \quad (92)$$

$$p_2(z, L) = 3H_{2a}(m^2) + \frac{3}{4} H_{2b}(m^2) + \frac{1}{3\hat{p}_*^2} [J_2(m^2, p_*) - J_2(m^2, 0)]. \quad (93)$$

We now finally change from the expansion of g in powers of g_0 to the one of \tilde{g} in \tilde{g}_0 of (20) with the corresponding coefficients. Some straightforward steps lead to

$$\tilde{q}_1 = r^{-2} q_1, \quad \tilde{q}_2 = r^{-4} q_2 + \frac{r^{-3}}{4} q_1^2 \quad (94)$$

and

$$\tilde{p}_1 = r^{-2} p_1 + \frac{r}{4} \tilde{q}_1, \quad \tilde{p}_2 = r^{-4} p_2 + \frac{r^{-1}}{2} p_1 \tilde{q}_1 + \frac{r}{4} \left(\tilde{q}_2 + \frac{r}{16} \tilde{q}_1^2 \right) \quad (95)$$

with the mass m in all arguments here.

B Small z expansion

By straightforward manipulations one can show that

$$\langle \bar{\phi}^m \rangle = \frac{\langle \bar{\phi}^m P(\bar{\phi}) \rangle_{0, \bar{\phi}}}{\langle P(\bar{\phi}) \rangle_{0, \bar{\phi}}} \quad (96)$$

holds with a polynomial in $\bar{\phi}$ deriving from

$$P(\bar{\phi}) = P_0(\bar{\phi}) \langle e^{-S_1} \rangle_{0, \eta} \quad (97)$$

truncated at the desired order in $g_0^{1/2}$. The subscripts of the averages refer to the parts of the action (35), (36) used. To construct P we perform Wick contractions with the η propagator

$$\tilde{\Delta}_0(p) = \frac{1}{\hat{p}^2 + g_0^{1/2}(2z_0^2 + \bar{\phi}^2)/(2L^2)}, \quad \Delta_0(x) = \frac{1}{L^4} \sum_{p \neq 0} e^{ipx} \tilde{\Delta}_0(p), \quad (98)$$

which will be expanded in $g_0^{1/2}$ in the end. The factor P_0 derives from the Gaussian integral over $e^{-S_{0, \eta}}$ and is given by

$$\ln P_0 = \frac{1}{2} \sum_{k \geq 1} \frac{(-1)^k}{k 2^k} g_0^{k/2} (2z_0^2 + \bar{\phi}^2)^k C_k(L) \quad (99)$$

with

$$C_k = L^{-2k} \sum_{p \neq 0} \frac{1}{(\hat{p}^2)^k}. \quad (100)$$

The dependence of C_k on L will be discussed in more detail below. By computing connected graphs we obtain in addition

$$\ln[P/P_0] = -\frac{g_0}{8} X^2 + \frac{g_0^{3/2}}{12} \bar{\phi}^2 L^2 \widetilde{\Delta}_0^3(0) + \frac{g_0^2}{48} \left[L^4 \widetilde{\Delta}_0^4(0) + 3X^2 \widetilde{\Delta}_0^2(0) \right] + O(g_0^{5/2}) \quad (101)$$

with the same notation as in the (78) and the short hand

$$X = L^2 \Delta_0(0) = \sum_{k \geq 1} C_k \left[-\frac{g_0^{1/2}}{2} (2z_0^2 + \bar{\phi}^2) \right]^{k-1}. \quad (102)$$

To compute the mass in a similar fashion we expand

$$\langle \hat{p}_*^2 \tilde{\Delta}(p_*) e^{-S_1} \rangle_{0, \eta} = P(\bar{\phi}) \times Q(\bar{\phi}) \quad (103)$$

with Q built from connected diagrams with two external lines at $p = \pm p_*$,

$$Q = Y - \frac{g_0}{2K_L}XY^2 + \frac{g_0^{3/2}}{2K_L}Y^2\bar{\phi}^2\widetilde{\Delta}_0^2(p_*) + \frac{g_0^2}{12K_L}Y^2 \times \\ \left[2L^2\widetilde{\Delta}_0^3(p_*) + 3X\widetilde{\Delta}_0^2(0) + 3X^2Y/K_L \right] + O(g_0^{5/2}) \quad (104)$$

with

$$Y = \hat{p}_*^2\widetilde{\Delta}_0(p_*) = \sum_{n \geq 0} \left[-\frac{g_0^{1/2}}{2K_L}(2z_0^2 + \bar{\phi}^2) \right]^n \quad (105)$$

evaluated up to the required order. We introduce additional constants for

$$L^{2k-4}\widetilde{\Delta}_0^k(0) = D_k + g_0^{1/2}(2z_0^2 + \bar{\phi}^2)D'_k + O(g_0), \quad [\Rightarrow D_2 \equiv C_2] \quad (106)$$

and

$$L^{2k-4}\widetilde{\Delta}_0^k(p_*) = D_k^* + g_0^{1/2}(2z_0^2 + \bar{\phi}^2)D_k^{*'} + O(g_0). \quad (107)$$

They are given by

$$D_k = L^{-2k} \sum_{p_1, \dots, p_k \neq 0} \delta_{\sum_i p_i, 0} \prod_{j=1}^k \frac{1}{\hat{p}_j^2} \quad (108)$$

and

$$D'_k = -\frac{k}{2}L^{-2k-2} \sum_{p_1, \dots, p_k \neq 0} \delta_{\sum_i p_i, 0} \frac{1}{(\hat{p}_1^2)^2} \prod_{j=2}^k \frac{1}{\hat{p}_j^2} \quad (109)$$

and corresponding formulas for D_k^* and $D_k^{*'}$ with p_* replacing zero for the total momentum. We now discuss the behavior of these constants as far as they enter into our computation.

We first note that there are a number of universal logarithmic divergences that enter into our final expansion coefficients B_k , like

$$L \frac{\partial}{\partial L} C_2 = L \frac{\partial}{\partial L} D_2 = \frac{1}{8\pi^2} + O(L^{-2}) = L \frac{\partial}{\partial L} D_2^*. \quad (110)$$

The constants D_3 and D_3^* are quadratically divergent, but their difference obeys

$$L \frac{\partial}{\partial L} (D_3 - D_3^*) = \frac{1}{64\pi^2} + O(L^{-2}). \quad (111)$$

Another combination that was found to occur in our final result is

$$L \frac{\partial}{\partial L} \left(C_2^2 + \frac{4}{3} D_3' \right) = -\frac{1}{64\pi^4} + O(L^{-2}). \quad (112)$$

All other constants are non-universal (reflect the hypercubic lattice and the discretization) and are either divergent ($C_1, D_4, D_3 + D_3^*$) or finite. They all drop out in our finite universal results for the β function. The behavior claimed above was checked by computing the constants numerically in the same way as reported in the previous appendix. However, the universal coefficients, which are the only feature needed here, should also be computable more easily in the continuum.

We are now ready to compute

$$\frac{z^2}{1 + z^2/K_L} = g_0^{1/2} \frac{\langle P(\bar{\phi})Q(\bar{\phi}) \rangle_{0,\bar{\phi}}}{\langle P(\bar{\phi})\bar{\phi}^2 \rangle_{0,\bar{\phi}}} \quad (113)$$

and g/z^4 from (42) and (96). We have implemented all the series in `maple` [with independent codes in Berlin and Munich] and obtain the corresponding truncated series in $g_0^{1/2}$ with coefficients given above and in terms of the moments

$$\mu_m = \langle \bar{\phi}^m \rangle_{0,\bar{\phi}}, \quad \mu \equiv \mu_2. \quad (114)$$

Derivatives with respect to z_0^2 are taken with the help of

$$\frac{\partial}{\partial z_0^2} \mu_m = -\frac{1}{2}(\mu_{m+2} - \mu_m \mu_2). \quad (115)$$

Partial integration implies

$$\mu_{m+4} + 6z_0^2 \mu_{m+2} - 6(m+1)\mu_m = 0 \quad (116)$$

which allows us to express all moments by $\mu = \mu_2$ in the final result. In this way we have arrived at the coefficients quoted under (63), (65), (66) and (67).

For $z_0^2 > 0$ the integral with (35) can be found under 3.323 in [11] and yields the result

$$\mu = 3z_0^2 \left(\frac{K_{3/4}(3z_0^4/4)}{K_{1/4}(3z_0^4/4)} - 1 \right) \quad (117)$$

with the modified Bessel function $K_\nu(\cdot)$ of index ν . For moderately negative z_0^2 we have simply summed the expansion for the integrals in z_0^2 to sufficiently high order. To compare with ordinary perturbation theory we need the perturbative expansion of μ for large z_0^2 ,

$$\mu = \frac{1}{z_0^2} - \frac{1}{2z_0^6} + \frac{2}{3z_0^{10}} - \frac{11}{8z_0^{14}} + \frac{34}{9z_0^{18}} + \mathcal{O}(z_0^{-22}). \quad (118)$$

In fact this is a nice pedagogical example for the working of an asymptotic series. In Fig. 7 we see the exact μ of (117) together with various truncations of the series (118). There is a range around $z_0^{-2} \gtrsim 1$ where the leading order alone is the most decent approximation, a situation reminiscent of the behavior of the perturbative series in Fig. 4.

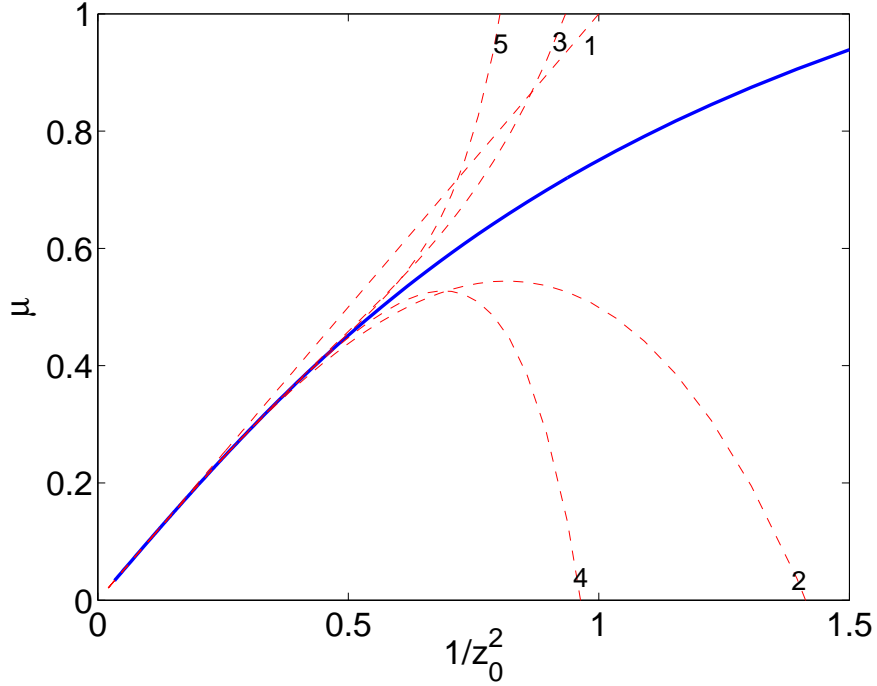


Figure 7: The behavior of μ from (117) and its perturbative approximations.

References

- [1] E. Brezin, J. C. Le Guillou, J. Zinn-Justin, Field Theoretical Approach to Critical Phenomena in *Phase Transitions and Critical Phenomena*, Vol.6, London 1976, 125.
- [2] M. Lüscher, P. Weisz, Scaling Laws and Triviality Bounds in the Lattice ϕ^4 Theory. 1. One Component Model in the Symmetric Phase, Nucl. Phys. B290 (1987) 25.
- [3] U. Wolff, Precision check on triviality of ϕ^4 theory by a new simulation method, Phys. Rev. D79 (2009) 105002.
- [4] I. Montvay, G. Münster, U. Wolff, Percolation Cluster Algorithm and Scaling Behavior in the four-dimensional Ising Model, Nucl. Phys. B305 (1988) 143.
- [5] M. Aizenman, Proof of the Triviality of ϕ^4 in D-Dimensions Field Theory and Some Mean Field Features of Ising Models for $D > 4$, Phys. Rev. Lett. 47 (1981) 1.

- [6] J. L. Lebowitz, GHS and other inequalities, Commun. Math. Phys. 35 (1974) 87.
- [7] M. Lüscher, P. Weisz, U. Wolff, A Numerical Method to compute the running Coupling in asymptotically free Theories, Nucl. Phys. B359 (1991) 221.
- [8] M. Lüscher, R. Narayanan, P. Weisz, U. Wolff, The Schrödinger Functional: A renormalizable Probe for non-Abelian Gauge Theories, Nucl. Phys. B384 (1992) 168.
- [9] E. Brezin, J. Zinn-Justin, Finite Size Effects in Phase Transitions, Nucl. Phys. B257 (1985) 867.
- [10] A. Bode, P. Weisz, U. Wolff, Two loop Computation of the Schrödinger Functional in Lattice QCD, Nucl. Phys. B576 (2000) 517.
- [11] I. S. Gradshteyn, I. M. Ryzhik, Table of Integrals, Series, and Products, Academic Press, Boston, 1980.